Scaled Quantum Mechanical Force Fields and Vibrational Spectra of Nucleic Acid Constituents. 9. Tetrahydrofuran

Marek Štrajbl,[†] Vladimír Baumruk,[†] and Jan Florián*,[‡]

Institute of Physics, Charles University, Ke Karlovu 5, 121 16 Prague 2, Czech Republic, and Department of Chemistry, University of Southern California, Los Angeles, California 90089-1062

Received: August 29, 1997

Infrared and Raman spectra of 1 M aqueous solution of tetrahydrofuran (THF) were recorded in the 850−3050 and 560−3050 cm^{-1} frequency range, respectively. The effects of hydrogen bonding on vibrational spectra of THF were analyzed by comparing spectra of aqueous solution with the spectra of liquid and solid THF reported previously by Cadioli et al. [*J. Phys. Chem.* **1993**, *97*, 7844]. More regular band shapes and smaller bandwidths of ring stretching modes indicate that the barrier for pseudorotation of the furanose ring increases in aqueous solution. This finding is in agreement with the results of our ab initio calculations using the Langevin dipoles (LD) solvation model, which predicted that the pseudorotational barrier of gaseous THF increases in aqueous solution by 0.25 ± 0.1 kcal/mol. Considering available gas-phase data, the free energy barrier for the pseudorotation in aqueous solution was estimated to be 0.5 ± 0.2 kcal/mol. The geometric structure and harmonic force fields of the C_2 conformer of THF were calculated by using the Hartree−Fock (HE), density functional theory (DFT), and Møller−Plesset perturbation theory of the second order (MP2). The scale factors for the S-VWN, B3-LYP and B-LYP density functional, and HF force constants of THF were determined. These scaled force fields were found to reproduce the observed frequencies with the overall 1% accuracy, with the B3-LYP method providing the most accurate results. The obtained agreement between the calculated and experimental infrared intensities, nonresonant Raman intensities, and depolarization ratios supports the proposed spectral assignment. The scale factors calculated here for THF augment scale factors determined previously for other nucleotide components: dimethyl phosphate and nucleic acid bases. Consequently, reliable ab initio interpretations of the vibrational spectra of nucleic acids in aqueous solution can be obtained in the future by using the concept of the transferability of scale factors from these nucleic acid constituents.

Introduction

Structure and dynamics of nucleic acids represent an important link between the molecular and biological levels of the organization of the living matter. Traditionally, IR and Raman spectroscopy has served as the basic experimental technique for the investigation of nucleic acids in their natural environment—aqueous solution.[1−4] Later, applications of other complementary vibrational spectroscopy methods such as resonance Raman spectroscopy,[3] vibrational circular dichroism (VCD),[5,6] and Raman optical activity (ROA)[7] to biomolecules dissolved in H_2O or D_2O emerged. In order to fully utilize the capabilities of these experimental methods, reliable theoretical approaches are highly needed to relate the obtained spectral information with the structural properties of the studied molecules.

A modern approach to the interpretation of the vibrational spectra involves the use of the scaled quantum mechanical (SQM) force fields[8] along with the IR absorption and Raman intensities evaluated by ab initio or density functional methods.[9−11] Scale factors for the SQM force fields incorporate the mean effect of the polar environment and compensate for the systematic errors of the ab initio or DFT force constants. After a basic calibration step, in which scale factors are adjusted based on the experimental data from simple model compounds, the assumption of the transferability of these scale factors to related molecules is made.

In the present work we carry out such a calibration step for tetrahydrofuran (THE), which represents the simplest model system for the vibrations of the furanose ring of ribose and deoxyribose embedded in the nucleic acid backbones. In addition, original nonresonant Raman and IR spectra of aqueous solutions of THF are presented, and the environmental effects on the vibrational spectra of THF are discussed. Finally, to obtain a deeper insight into the properties of THF in aqueous solution, we evaluated the hydration effects on the pseudorotation barrier of THF.

Methods

Experimental Raman spectra of 1 M aqueous solution were recorded on a multichannel spectrometer based on a liquid nitrogen cooled CCD detection element (EEV) having 1024 pixels along the dispersion axis. Spectra were excited with a 514.5 nm line of an argon laser (Coherent Innova 305) with 200 mW of radiant power at a sample. The spectral slit width was ca. 5 cm^{-1}.

Infrared spectra were recorded with a Nicolet Impact 400 FTIR spectrometer using a standard source, a KBr beam splitter,

[†] Charles University.
[‡] University of Southern California.

S1089-5647(97)02829-0 CCC: $15.00
Published on Web 01/23/1998

TABLE 1: Definition of Internal Coordinates of Tetrahydrofuran

coordinate[a]	description	definition[b]
νO1C1	OC stretching	$\Delta r_{O1,C1}$
νC1C2	C1C2 stretching	$\Delta r_{C1,C2}$
νC2C3	C2C3 stretching	$\Delta r_{C2,C3}$
νC1Hs	CH_2 sym stretching	$\sqrt{2}/2(\Delta r_{C1,H11} + \Delta r_{C1,H12})$
νC1Ha	CH_2 asym stretching	$\sqrt{2}/2(\Delta r_{C1,H11} - \Delta r_{C1,H12})$
δC1Hs	CH_2 sym bending	$\Delta\alpha_{H11,C1,H12}$
δC1Hr	CH_2 rocking	$1/2(\Delta\alpha_{H11,C1,C2} - \Delta\alpha_{H12,C1,C2} + \Delta\alpha_{H11,C1,O1} - \Delta\alpha_{H12,C1,O1})$
δC1Hw	CH_2 wagging	$1/2(\Delta\alpha_{H11,C1,C2} + \Delta\alpha_{H12,C1,C2} - \Delta\alpha_{H11,C1,O1} - \Delta\alpha_{H12,C1,O1})$
δC1Ht	CH_2 twisting	$1/2(\Delta\alpha_{H11,C1,C2} - \Delta\alpha_{H12,C1,C2} - \Delta\alpha_{H11,C1,O1} + \Delta\alpha_{H12,C1,O1})$
δRA	ring bending	$0.63245\Delta\alpha_{C4,O1,C1} - 0.51167(\Delta\alpha_{O1,C1,C2} + \Delta\alpha_{C3,C4,O1}) + 0.19544\ (\Delta\alpha_{C1,C2,C3} + \Delta\alpha_{C2,C3,C4})$
δRB		$0.37175(\Delta\alpha_{C3,C4,O1} - \Delta\alpha_{O1,C1,C2}) + 0.60150(\Delta\alpha_{C1,C2,C3} - \Delta\alpha_{C2,C3,C4})$
τRA	ring torsion	$0.19544(\Delta\tau_{C4,O1,C1,C2} + \Delta\tau_{C3,C4,O1,C1}) - 0.51167(\Delta\alpha_{O1,C1,C2,C3} + \Delta\tau_{C2,C3,C4,O1}) + 0.63245\Delta\tau_{C1,C2,C3,C4}$
τRB		$0\ 37175\ (\Delta\tau_{O1,C1,C2,C3} - \Delta\tau_{C2,C3,C4,01}) + 0.60150(\Delta\tau_{C3,C4,O1,C1} + \Delta\tau_{C4,O1,C1,C2})$

[a] Coordinates observing local symmetry. Only coordinates for the structurally unique part of the molecule are given. The definition of internal coordinates for the other part of the molecule was done analogously. [b] The symbols r, α, and τ denote bond length, bond angle, and torsional angle, respectively. For atom numbering see Figure 1.

and a DTGS detector. Generally, 256 scans were coadded with a spectral resolution of 4 cm^{-1} and a Happ-Genzel apodization function. The sample was placed in a demountable cell (Specac) consisting of a pair of ZnSe windows separated by a 15 μm Teflon spacer.

Ab initio geometry optimizations and harmonic force field calculations of the C_2 conformer of tetrahydrofuran were carried out by using the Gaussian 94 program.[12] We used the Hartree−Fock (HF) approximation, the second-order Møller−Plesset perturbation theory (MP2), and the density functional theory (DFT). Standard Gaussian polarized split-valence basis sets, 6-31G* and 6-31+G**, were used. Three types of functionals were considered in the DFT calculations. These included the local S-VWN[13] functional, the combination of the nonlocal Becke's exchange functional[14] and Lee−Yang−Parr correlation functional (B-LYP),[15] and the hybrid B3-LYP functional[16] that consists of the HF and nonlocal exchange and correlation parts.

IR and Raman spectra were computed using the harmonic approximation. Because the calculation of the polarizability derivatives by the DFT and MP2 methods was not implemented in the Gaussian 94 program, we calculated Raman intensities by combining the SQM force fields with polarizability derivatives obtained at the HF level with the 6-31++G** basis set. The computer programs MOLVIB[17] and SQMVIB[18] were used for the calculation of the vibrational spectra and scaling procedure. First, the ab initio Cartesian force-constant matrix was transformed into standard internal coordinates observing local symmetry[8] (Table 1). The force constants were then scaled by scale factors adjusted by minimizing the difference between the calculated and observed vibrational frequencies. The τRB force constant that is closely related to the pseudorotational deformation of the five-membered ring was left unscaled. We used the geometric-mean scaling.[8] In this approach, the interaction (off-diagonal) force constants are scaled (multiplied) by the square root of the product of the scale factors belonging to the corresponding diagonal force constants: $S_{ij} = (S_{ii}S_{jj})^{1/2}$. In this way, four sets of scale factors were independently determined for the HF and DFT force fields obtained by using the 6-31G* basis set. The force constants calculated at the MP2 level and with the larger 6-31+G** basis set were used to check accuracy and the basis set dependence of the HF and DFT/6-31G* force fields. An expression based on the double-harmonic nonresonant approximation was used for the evaluation of IR intensities and Raman differential cross sections.[9,19,20] Right-angle scattering geometry with exciting light polarized perpendicularly to the scattering plane, no analyzer, 488 nm excitation wavelength, and temperature 300 K were assumed in the intensity calculations.

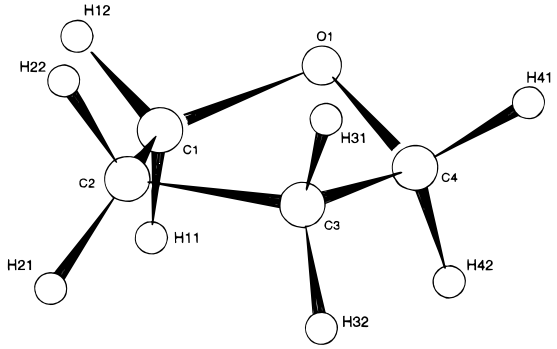

Figure 1. Atom numbering of a molecule of tetrahydrofuran (THF).

Solvation free energies were calculated by using the Langevin dipoles (LD)[21−23] and polarized continuum (PCM)[24,25] solvation models. The LD model evaluates an average polarization of the solvent molecules surrounding the solute by using the discrete dipolar representation of the solvent and the arbitrary-shape solute−solvent boundary formed by the atom-centered intersecting spheres. The ab initio version of the LD model[23] was recently parametrized to reproduce experimental solvation energies of a representative set of small neutral and ionic molecules. This model uses the electrostatic potential-derived atomic charges to represent the charge distribution of the solute molecules. The LD calculations were carried out for the HF/6-31G* and B3-LYP/6-31G* geometries and charge distributions of the C_2 and C_s stationary points[26] by using the program ChemSol.[23,27] The contributions to the solvation free energy due to the solute polarization by the solvent (induction effects) are included in the calculated solvation free energies by using solute charges evaluated in the presence of the continuum dielectric ($\epsilon = 80$) surrounding the solute. To calculate these solvated atomic charges as well as for independent calculations of solvation free energies, the Gaussian 94[12] implementation of the PCM model was used. The default Pauling's atomic radii multiplied by a factor of 1.2 were used in these PCM calculations.

Results and Discussion

Tetrahydrofuran (THF, Figure 1) is a highly flexible molecule with the very low barrier to *pseudorotation*.[28] In this type of ring puckering, the position of the maximum displacement from the mean plane of the ring travels around the five-membered ring from one ring atom to the next, while the sum of square

TABLE 2: Diagonal Force Constants[a] of C_2 Conformation of Tetrahydrofuran

coordinate[b]	hf[c]	svwn	svwn$^+$	blyp	blyp$^+$	b3lyp	b3lyp$^+$	mp2$^+$
νO1C1	6.199	5.345	5.149	4.395	4.182	5.016	4.834	4.954
νC1C2	4.983	4.588	4.532	4.012	3.955	4.355	4.300	4.697
νC2C3	4.875	4.561	4.482	3.948	3.862	4.299	4.219	4.590
νC1Hs	5.851	4.897	4.905	4.867	4.890	5.175	5.175	5.487
νC1Ha	5.669	4.756	4.781	4.693	4.733	5.008	5.022	5.390
νC2Hs	5.879	5.110	5.079	5.029	5.008	5.312	5.279	5.560
νC2Ha	5.746	5.049	5.029	4.923	4.911	5.207	5.183	5.518
δC1Hs	0.936	0.766	0.734	0.793	0.760	0.824	0.794	0.829
δC1Hr	1.054	0.879	0.844	0.898	0.861	0.933	0.901	0.926
δC1Hw	0.910	0.728	0.711	0.751	0.734	0.785	0.770	0.790
δC1Ht	0.809	0.652	0.639	0.653	0.641	0.692	0.680	0.694
δC2Hs	0.880	0.709	0.685	0.748	0.724	0.775	0.752	0.779
δC2Hr	0.746	0.598	0.587	0.637	0.628	0.658	0.649	0.667
δC2Hw	0.804	0.637	0.621	0.664	0.647	0.693	0.677	0.700
δC2Ht	0.798	0.657	0.638	0.668	0.649	0.698	0.680	0.702
δRA	1.315	1.139	1.124	1.132	1.115	1.178	1.163	1.177
δRB	0.780	0.645	0.638	0.643	0.634	0.676	0.669	0.687
τRA	0.181	0.211	0.203	0.164	0.156	0.170	0.163	0.201
τRB	0.011	0.014	0.013	0.010	0.009	0.010	0.010	0.012

[a] Stretching and bending force constants are given in mdyn/Å and mdyn Å, respectively. [b] For definition of internal coordinates see Table 1. [C] Computational methods are abbreviated as follows: hf = HF/6-31G*, svwn = SVWN/6-31G*, svwn$^+$ = SVWN/6-31+G**, blyp = BLYP/6-31G*, blyp$^+$ = BLYP/6-31+G**, b31yp = B3LYP/6-31G*, b31yp$^+$ = B3LYP/6-31+G**, mp2$^+$ = MP2/6-31+G**.

TABLE 3: Scale Factors for the Diagonal Force Constants[a] of THF

internal coord[b]	hf	svwn	blyp	b3lyp
OC stretching	0.685	0.805	1.025	0.876
CC stretching	0.887	0.952	1.099	1.012
CH stretching	0.817	0.956	0.970	0.914
CH bending	0.784	1.015	0.981	0.925
ring bending	0.867	1.065	1.067	0.998
τRA	1.215	1.047	1.413	1.352

[a] For notation of computational methods see captions of Table 2. [b] For definition of internal coordinates see Table 1.

displacements of the five ring atoms remains approximately constant.[29] The pseudorotational path connects the two symmetrically equivalent conformers of C_2 symmetry that correspond to the global minima on the potential energy surface.[28] In these C2-endo and C3-endo conformers, the C2 and C3 atoms are equally displaced from the C1O1C4 plane. The transition state on this minimum-energy pathway possesses the C_s symmetry and corresponds to the envelope conformation, in which all carbon atoms lie in a common plane and the oxygen atom is displaced above or below this plane. As an anharmonic large-amplitude motion, pseudorotation precludes the identification of the fundamental vibrational modes in the spectrum of gaseous THF[28] and superimposes a complicated fine structure on the fundamental bands in the IR spectrum of the liquid and solid THF.[28,30] Aqueous solvation is a natural interaction in biochemistry, and in the case of THF it was predicted to stabilize the C_2 conformation.[26] Therefore, the C_2 conformer of THF and spectra measured from aqueous solution were chosen by us to be a structural and experimental basis of the scale factor determination.

The geometric structure of THF has been studied by the microwave spectroscopy,[31] electron, X-ray, and neutron diffraction,[32−34] and also correlated ab initio calculations.[26,28] The diagonal *force constants* of the C_2 conformer obtained at several computational levels are compared in Table 2. Here, one can note a negligible basis set dependence of the diagonal force constants calculated by using DFT methods. In addition,

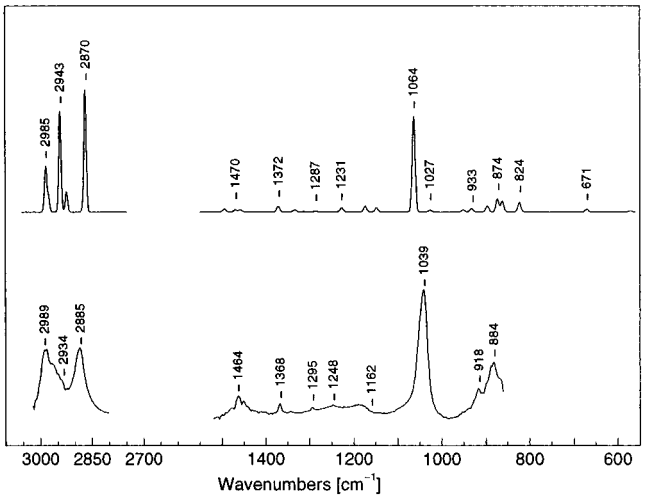

Figure 2. (top) Calculated (SQM B3-LYP/6-31G*) spectra of THF. (bottom) IR spectra of 1 M H_2O solution of THF.

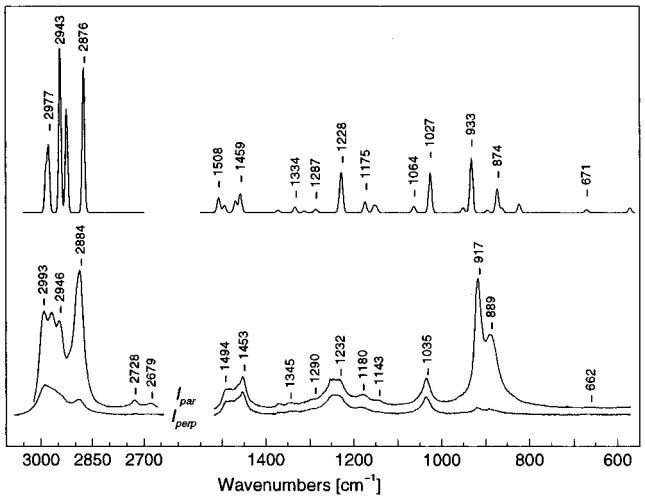

Figure 3. (top) Calculated (SQM B3-LYP/6-31G*) Raman spectra of THF. (bottom) Polarized Raman spectra of 1 M H_2O solution of THF.

these methods were previously shown to provide reliable geometrical structures[35,36] and off-diagonal force constants.[37,38] Therefore, HF and DFT calculations with a modest 6-31G* basis set were chosen by us as most suitable methods for predicting vibrational properties of nucleic acids. Currently, relatively large systems such as nucleobase dimers[39] and trimers[40] can be treated at this computational level. Moreover, due to recent advances in computational methodology,[41,42] short oligonucleotides can be investigated by the HF and DFT methods in near future.

The *scale factors* developed by us for the HF, S-VWN, B3-LYP, and B-LYP force fields are presented in Table 3. These scale factors cover all the local structural features of THF that are preserved in nucleic acids. However, the number of these empirical parameters is small enough so that they could be unambiguously determined using experimental frequencies from IR and Raman spectra of aqueous solution of THF. The concept of the transferability of these scale factors can be illustrated by comparing the HF/6-31G* scale factors obtained for the structurally similar chemical groups in THF (Table 3), dimethyl phosphate (DMP),[20] and cytosine.[43] For example, CH stretching vibrations are generally independent of their chemical environment. Consequently, the CH stretching scale factors in THF, DMP, and cytosine are 0.817, 0.805, and 0.81, respectively. The degree of similarity decreases for CH bending vibrations

TABLE 4: Experimental and Calculated Vibrational Spectra of Tetrahydrofuran in Aqueous Solution

frequency (intensity)[a]				depolarization ratio			
IR[b]	Raman[b]	hf[c]	b3lyp[d]	expt	hf	b3lyp	assignment (PED (%))[e]
140[f]		70 (6.8, 0.2)	45 (4.2, 0.3)		0.75	0.75	τRB(57), δCHt(26)
286[f]		284 (0.0, 2.5)	289 (0.0, 5.0)	0.75	0.74	0.75	τRA(85)
	587 vw	568 (0.8, 20)	572 (1.1, 15)		0.75	0.75	δRB(50), δCHr(36)
	662 vw	668 (4.1, 9.4)	671 (3.2, 9.2)		0.75	0.68	δRA(63), δCHr(16)
	840[f]	815 (21, 37)	824 (12, 26)	p	0.15	0.17	ν_sOC(28), δCHr(24)
866 sh		854 (19, 23)	863 (14, 14)		0.75	0.75	δCHr(48), ν_aOC(24) − δRB(18)
884 s	889 s	860 (14, 59)	874 (16, 74)	0.05	0.22	0.16	ν_sOC(62), δCHr(12)
900 sh		892 (11, 7.8)	897 (7.4,7.6)		0.75	0.75	δCHt(40), ν_aCC(24)
918 m	917 vs	925 (5.7, 136)	933 (4.3, 164)	0.04	0.07	0.06	νC2C3(50) + ν_sCC(36)
954 w		944 (4.2, 20)	952 (2.4, 14)		0.75	0.75	ν_aCC(28), δCHr(34)
	1035 m	1018 (3.1, 131)	1027 (2.2, 123)	0.63	0.72	0.72	ν_sCC(30) − νC2C3(14), δCHw(24)
1039 vs		1077 (150, 9.9)	1064 (117, 20)	0.75	0.75	0.75	ν_aOC(58) + δRB(18)
1048 sh	1053 sh						combination band (917 + 140)
1141 vw	1143 w	1155 (0.1, 22)	1155 (0.0, 20)	0.18	0.57	0.29	δCHr(82)
1162 vw		1159 (7.6, 11)	1149 (5.0, 14)		0.75	0.75	δCHt(44), δCHr(30)
1190 br	1180 w	1189 (8.7, 53)	1175 (7.1, 34)	0.60	0.72	0.65	δCHt(32), νC2C3(16) − δRA(12)
1222 w							combination band (917 + 286)
1231 w	1232 m	1231 (3.5, 125)	1228 (4.7, 82)	0.72	0.75	0.75	δCHt(82)
1248 m	1252 m	1232 (0.3, 69)	1231 (0.5, 54)	0.70	0.71	0.68	δCHt(68), δCHr(12)
1295 m	1290 w	1293 (1.1, 12)	1287 (1.0, 11)	0.75	0.75	0.75	δCHw(94)
1312 w		1323 (1.4, 3.3)	1313 (0.3, 4.2)		0.74	0.75	δCHw(52), δCHt(22), νC2C3(12)
1345 w	1345 w	1347 (2.8, 21)	1334 (2.6, 17)	0.72	0.75	0.75	δCHw(82)
1368 m	1371 w	1383 (11, 9.5)	1372 (7.0, 7.4)	0.36	0.31	0.30	δCHw(82)
1452 m	1453 s	1448 (2.3, 80)	1459 (2.6, 58)	0.75	0.75	0.75	δCHs(96)
1464 m	1468 sh	1461 (2.4, 51)	1470 (2.5, 36)	0.75	0.74	0.74	δCHs(86)
1478 m	1482 m	1490 (4.3, 29)	1495 (3.6, 23)	0.77	0.75	0.75	δCHs(98)
1492 w	1494 m	1502 (0.4, 67)	1508 (0.1, 45)	0.60	0.66	0.66	δCHs(88)
	2679 w			0.41			overtone (2 × 1345)
	2728 w			0.16			overtone (2 × 1371)
2885 s		2893 (145, 26)	2870 (150, 22)		0.75	0.75	νCHs(72), νC4Ha(26)
	2884 vs	2897 (15, 294)	2876 (5.2, 455)	0.09	0.22	0.20	νCHs(66), νC4Ha(32)
2897 sh	2896 sh			0.09			overtone (2 × 1453)
	2915 sh	2911 (19, 280)	2924 (22, 241)	0.28	0.23	0.28	νCHs(68), νC4Ha(18)
2920 m		2912 (27, 65)	2927 (4.6, 109)		0.75	0.75	νCHs(76), νC4Ha(12)
2934 sh		2950 (108, 76)	2943 (123, 37)		0.75	0.75	νCHa(60), νC4Hs(22)
2949 sh	2946 s	2953 (2.6, 353)	2944 (2.5, 485)	0.22	0.18	0.16	νCHa(58), νC4Hs(26)
2965 sh	2970 s	2959 (32, 172)	2977 (19, 208)	0.27	0.44	0.29	νCHa(80), νC4Hs(18)
2989 s	2993 s	2969 (107, 116)	2985 (56, 140)	0.32	0.75	0.75	νCHa(94)

[a] Frequency (cm^{-1}) (IR intensity (km/mol), Raman differential cross section (10^{-36} m^2 sr^{-1})). Experimental intensities are abbreviated as vs (very strong), s (strong), m (medium), w (weak), vw (very weak), sh (shoulder). [b] Vibrational spectra of 1 M aqueous solution at 300 K. [c] SQM HF/6-31G* force field. [d] SQM B3-LYP/6-31G* force field. Raman differential cross sections were calculated from the b31yp normal modes combined with the HF/6-31++G**//B3-LYP/6-31G* Cartesian polarizability derivatives. [e] Calculated by using the SQM B3-LYP/6-31G* force field. Potential energy distribution (PED) for CH vibrations is given in terms of total contributions from all $-CH_2-$ groups. For the corresponding internal coordinates see Table 1. For the ring stretching vibrations, C_2 symmetry coordinates are defined as follows: ν_sOC = νO1C1 + νO4C4, ν_aOC = νO1C1 − νO4C4, ν_sCC = νC1C2 + νC3C4, ν_aCC = νC1C2 − νC3C4. [f] From ref 28, IR and Raman spectra of liquid THF at 298 K.

of methylene (THF), methyl (DMP), and H−C(sp^2) (cytosine) groups, for which scale factors 0.784, 0.84, and 0.88 were obtained. Furthermore, the CC and CO bonds that are part of THF and cytosine are structurally different. Thus, the CC and CO scale factors in these two molecules largely differ. Finally, force constants of CO single bonds in the cyclic (THF) and acyclic (DMP) arrangements were found to have similar scale factors.

The use of the SQM B3-LYP/6-31G* force field resulted in the 9 cm^{-1} root-mean-square (rms) difference between the observed and calculated frequencies. This method slightly outperformed its B-LYP and HF counterparts. The largest rms error (12 cm^{-1}) was obtained for the SQM S-VWN/6-31G* force field.

Experimental and calculated *IR and Raman spectra* of 1 M aqueous solution of THF are presented in Figures 2 and 3 and in Table 4. These spectra are interpreted in Table 4 by using the SQM B3-LYP/6-31G* potential energy distribution (PED). This assignment was found to be nearly the same as our SQM HF/6-31G* and B-LYP/6-31G* results. Also, it is practically identical to the interpretation published recently by Cadioli et al.[28] Therefore, we will focus mainly on the discussion of the predicted IR and Raman intensities and the differences between the spectra of liquid THF and the spectra of its aqueous solution in the low-frequency (200−1800 cm^{-1}) region.

The calculated *IR intensities* reproduce well the observed spectrum, with the single strong peak (1039 cm^{-1}) corresponding to the antisymmetric CO stretching vibration (ν_aCO). Because the derivatives of the molecular dipole moment that determine the calculated IR intensities were obtained for the isolated THF molecule, the relative intensity of this mode is slightly underestimated compared with the spectrum measured from aqueous solution. Agreement slightly improves when the IR spectrum of THF liquid[28] is considered. Here, the ν_aCO bands shifts to 1070 cm^{-1}, its relative intensity decreases (though it still remains the strongest peak in the low-frequency part of the spectrum), and a weak 1032 cm^{-1} shoulder appears at its low-frequency side. The large frequency shift of the ν_aCO band upon going from the liquid to aqueous solution can be attributed to the hydrogen bonding between water molecules and the oxygen atom of THF. This interaction does not occur in liquid THF since THF does not have a proton donor group capable of

TABLE 5: Hydration Free Energies for the C_2 and C_s Conformers of THF

	ΔG_{solv} (kcal/mol)	
method[a]	C_2	C_s
LD/hf	−4.02	−3.79
LD/b3lyp	−3.18	−2.91
PCM/hf	−4.07	−3.94
PCM/b3lyp	−3.19	−3.08
experiment[b]	−3.5	

[a] hf and b3lyp denote HF/6-31G* and B3-LYP/6-3G* methods, respectively. [b]Reference 45.

forming hydrogen bonds. The observed frequency shift was not properly reproduced by the SQM method. This is because hydrogen bonding affects in a different way the frequencies of symmetric and antisymmetric CO stretching modes (see also below), and these trends cannot be properly modeled by using a single diagonal scale factor. Similar problems were noted by us for the PO stretching modes of phosphate groups.[20]

Due to the large demands on the quality of the basis set needed for accurate reproduction of the nonresonant *Raman intensities* by ab initio and DFT methods,[11] the agreement of the experimental and calculated Raman intensities is not optimal. Nevertheless, our calculations were able to identify strong spectral bands, and more importantly, they were able to provide quite accurate depolarization ratios. These results verify the proposed band assignment and establish the basis for meaningful theoretical interpretation of structure-related variations in measured depolarization ratios of biomolecules. As far as the method dependence of the calculated Raman intensities and depolarization factors is concerned, the larger basis set used for calculation of b31yp intensities (6-31++G**) resulted in a substantial improvement over the HF/6-31G* results (Table 4).

The low-frequency part of the Raman spectrum is dominated by two strong bands lying near 900 cm^{-1}. These bands belong to the symmetric (in-phase) stretching vibrations of the five-membered furanose ring. The position of the lower frequency component (889 cm^{-1}, ν_sCO) was found to be little influenced by aqueous solvation. As discussed in previous paragraph, the frequency of this mode is underestimated by our SQM calculations. The position of the other component (917 cm^{-1}) lies at a higher frequency (928 cm^{-1}) in the spectrum of liquid THF.[28] This band corresponds to the in-phase stretching of all CC bonds, and it is therefore often denoted as "breathing" vibration of the five-membered ring. While frequency separation of the ν_sCO and breathing modes decreases in aqueous solution compared to the spectra of THF liquid, they also become more narrow. We attribute this effect to the hydration-related increase in the pseudorotational barrier of THF.

This interpretation is in agreement with the results of the theoretical calculations that employed two different solvation models (Table 5). The calculated difference in *hydration free energies* ($\Delta\Delta G_{solv}$) between the C_s and C_2 conformations of THF is nearly independent of the ab initio method that was used to generate solute charge distribution. The largest contribution to this difference is due to the electrostatic component of ΔG_{solv}. The LD solvation model predicts slightly larger hydration effects than the PCM model. A similar trend was previously noted for ethanediol[23] and dimethyl phosphate.[44] We believe that the LD predictions of the conformational variations in hydration free energy are more reliable because this model treats correctly contributions to ΔG_{solv} from the solute charge density lying outside the solute−solvent boundary. Thus, using the LD value for $\Delta\Delta G_{solv}$ (0.25 ± 0.1 kcal/mol), the experimental value for the pseudorotational barrier in the gas phase (0.16 ± 0.03 kcal/mol)[31] and the zero-point vibrational energy correction (0.1 ± 0.05 kcal/mol),[26] the total free energy barrier for the pseudorotation of THF dissolved in aqueous solution can be estimated as 0.5 ± 0.2 kcal/mol. This barrier falls below the value of the average thermal energy at 300 K (0.6 kcal/mol), but it is large enough for the pseudorotational vibration of the C_2 conformer to be directly observable near 140 cm^{-1} as reported by Cadioli et al.[28]

Acknowledgment. This work was supported by the Grant Agency of the Czech Republic (Grant 203/93/2362). The calculations were carried out at the Supercomputing Center of Charles University and the Joint Supercomputing Center of Czech Technical University and University of Chemical Technology. The kind help of Prof. Ivan Barvík is gratefully acknowledged.

References and Notes

(1) Miles, H. T. *Methods Enzymol.* **1968**, *12B*, 256.
(2) Taillandier, E.; Liquier, J. *Methods Enzymol.* **1992**, *211*, 307.
(3) Peticolas, W. L.; Evertsz, E. *Methods Enzymol.* **1992**, *211*, 335.
(4) Thomas Jr., G. J.; Tsuboi, M. *Adv. Biophys. Chem.* **1993**, *3*, 1.
(5) Baumruk, V.; Keiderling, T. A. *J. Am. Chem. Soc.* **1993**, *115*, 6939.
(6) Maharaj, V.; Rauk, A.; Vandesande, J. H.; Wieser, H. *J. Mol. Struct.* **1997**, *408*, 315.
(7) Bell, A. F.; Hecht, L.; Barron, L. D. *J. Am. Chem. Soc.* **1997**, *119*, 6006.
(8) Fogarasi, G.; Pulay, P. In *Vibrational Spectra and Structure;* Durig, J. R., Ed.; Elsevier: Amsterdam, 1985; Vol. 14, p 125.
(9) Person, W. B. In *Vibrational Intensities in Infrared and Raman Spectroscopy;* Person, W. B., Zerbi, G., Eds; Elsevier: Amsterdam, 1982.
(10) Polavarapu, P. L. *J. Phys. Chem.* **1990**, *94*, 8106.
(11) Johnson, B. G.; Florián, J. *Chem. Phys. Lett.* **1995,** *247*, 120.
(12) Frisch, M. J.; Trucks, G. W.; Schlegel, H. B.; Gill, P. M. W.; Johnson, B. G.; Robb, M. A.; Cheeseman, J. R.; Keith, T.; Petersson, G. A.; Montgomery, J. A.; Raghavachari, K.; Al-Laham, M. A.; Zakrzewski, V. G.; Ortiz, J. V.; Foresman, J. B.; Cioslowski, J.; Stefanov, B. B.; Nanayakkara, A.; Challacombe, M.; Peng, C. Y.; Ayala, P. Y.; Chen, W.; Wong, M. W.; Andres, J. L.; Replogle, E. S.; Gomperts, R.; Martin, R. L.; Fox, D. J.; Binkley, J. S.; Defrees, D. J.; Baker, J.; Stewart, J. P.; Head-Gordon, M.; Gonzalez, C.; Pople, J. A. *Gaussian 94, Revision C.2;* Gaussian, Inc.: Pittsburgh, PA, 1995.
(13) Vosko, S. H.; Wilk, L.; Nusair, M. *Can. J. Phys.* **1980**, *58*, 1200.
(14) Becke, A. D. *Phys. Rev.* **1988**, *A38*, 3098.
(15) Lee, C.; Yang, W.; Parr, R. G. *Phys. Rev. B* **1988**, *37*, 785.
(16) Becke, A. D. *J. Chem. Phys.* **1993**, *98*, 5648.
(17) Sundius, T. *J. Mol. Struct.* **1990**, *218*, 321.
(18) Florián, J. *SQMVIB: A computer program for calculation of scaled quantum mechanical vibrational spectra of molecules;* Charles University: Prague, 1994.
(19) Amos, R. D. *Chem. Phys. Lett.* **1986**, *124*, 376.
(20) Florián, J.; Baumruk, V.; Strajbl, M.; Bednárová, L.; Stepánek, J. *J. Phys. Chem.* **1996,** *100*, 1559.
(21) Warshel, A. *J. Phys. Chem.* **1979**, *83*, 1640.
(22) Russell, S. T.; Warshel, A. *J. Mol. Biol.* **1985**, *185*, 389.
(23) Florián, J.; Warshel, A. *J. Phys. Chem. B* **1997**, *101*, 5583.
(24) Miertus, S.; Scrocco, E.; Tomasi, J. *Chem. Phys.* **1981**, *55*, 117.
(25) Miertus, S.; Tomasi, J. *Chem. Phys.* **1982**, *65*, 239.
(26) Strajbl, M.; Florián, J. *Theor. Chem. Acc.*, in press.
(27) Florián, J.; Warshel, A. *ChemSol, Version 1.0;* University of Southern California: Los Angeles, CA, 1997.
(28) Cadioli, B.; Gallinella, E.; Coulombeau, C.; Jobic, H.; G. B. *J. Phys. Chem.* **1993**, *97*, 7844.
(29) Altona, C.; Sundaralingam, M. *J. Am. Chem. Soc.* **1972**, *94*, 8205.
(30) Gallinella, E.; Cadioli, B.; Flament, J. P.; Berthier, G. *J. Mol. Struct.* **1994**, *315*, 137.
(31) Engerholm, G. G.; Luntz, A. C.; Gwinn, W. D.; Harris, D. O. *J. Chem. Phys.* **1969**, *50*, 2446.
(32) Geise, H. J.; Adams, W. J.; Bartell, L. S. *Tetrahedron* **1969**, *25*, 3045.
(33) Luger, P.; Buschmann, J. *Angew. Chem.* **1983**, *95*, 423.
(34) David, W. I. F.; Ibberson, R. M. *Acta Crystallogr.* **1992**, *C48*, 301.
(35) Fitzgerald, G.; Andzelm, J. *J. Phys. Chem.* **1991**, *95*, 10531.

(36) Johnson, B. G.; Gill, P. M. W.; Pople, J. A. *J. Chem. Phys.* **1993**, *98*, 5612.
(37) Florián, J.; Johnson, B. G. *J. Phys. Chem.* **1994**, *98*, 3681.
(38) Florián, J.; Leszczynski, J.; Johnson, B. G.; Goodman, L. *Mol. Phys.* **1997**, *91*, 439.
(39) Florián, J.; Leszczynski, J. *Int. J. Quantum Chem.: Quantum Biol. Symp.* **1995**, *22*, 207.
(40) Sponer, J.; Burda, J. V.; Mejzlik, P.; Leszczynski, J.; Hobza, P. *J. Biomol. Struct. Dyn.* **1997**, *14*, 613.
(41)) White, C. A.; Johnson, B. G.; Gill, P. M. W.; Head-Gordon, M. *Chem. Phys. Lett.* **1996**, *253*, 268.
(42) Strain, M. C.; Scuseira, G. E.; Frisch, M. J. *Science* **1996**, *271*, 51.
(43) Florián, J.; Baumruk, V.; Leszczynski, J. *J Phys. Chem.* **1996**, *100*, 5578.
(44) Florián, J.; Strajbl, M.; Warshel, A. Submitted for publication.
(45) Cabani, S.; Gianni, P.; Mollica, V.; Lepori, L. *J. Solution Chem.* **1981**, *10*, 563.